A High harmonic large orbit gyrotron in THz range

Xiang Li [*], Jiandong Lang, Yasir Alfadhl and Xiaodong Chen
School of Electronic Engineering and Computer Science
Queen Mary University of London
Mile End Road, London, United Kingdom, E1 4NS,
[*] Email: xiang.x.li@qmul.ac.uk

Abstract: A high-harmonic large orbit gyrotron (LOG) operating in the THz range has been designed and studied. Numerical simulations have shown that the 5th harmonic oscillation at 283 *GHz* can be selectively excited by proper choice of the external magnetic field and the electron beam current. The high harmonic operation of LOG is characterised by the considerable reduction of the required external magnetic field strength. The beam-wave interaction, the starting oscillation process and the ohmic loss of the designed LOG are also examined. The analysis procedure and the conclusion can form the basis for the study of even higher harmonics operation.

Keywords: Gyrotron, Harmonic resonance, Large orbit gyrotron (LOG), THz range.

1. Introduction

The gyrotron is one of the most promising high power millimetre wave and THz sources that form the foundation for many applications including plasma diagnostics [1], dynamic nuclear polarisation [2], deep-space and special satellite communications [3]. However, this device is not yet widely applied in THz range because the operation requires high external magnetic field. For example, to enable the oscillation of 0.3 *THz* at the fundamental electron cyclotron harmonic (s=1), the required magnetic field is as high as 10 *T*, which exceeds the capability of a number of gyrotrons laboratories. To fulfill the gap between the expected operation frequency and the available magnetic field intensity, harmonic operation becomes attractive because the required magnetic field intensity is inversely proportional to the operation harmonic number. Nevertheless, due to the complicated mode competition problem, operation of the traditional small-orbit gyrotron is limited within the first three harmonics. For higher harmonics operation, the conventional methods of mode competition suppression such as the beam positioning become insufficient. The mode competition problem will cause unstable output power level or low efficiency of the device.

To maintain single mode operation at high harmonics, a beam-wave dynamic system with much stronger selectivity of the cavity modes should be adopted. One of the leading candidates is the large orbit gyrotron (LOG) configuration where the guiding centre of the electrons is located on the axis of the waveguide. By this configuration, only modes with azimuthal index equal to the harmonic number can be excited [4-6]. By such restriction, the competition mode spectrum in

the cavity can be greatly rarefied. As a matter of fact, this feature has been applied in a number of experimental and numerical demonstrations of high harmonic LOG [4-7]. For example, the fifth harmonic operation has been experimentally verified at 138 *GHz* in University of Fukui [5]. And the seventh harmonic oscillation at 390 *GHz* has been observed numerically in University of Strathclyde while using a perfect electrical conductor (PEC) as the cavity wall [7].

In this paper, a LOG operating at the fifth harmonic of the electron cyclotron resonance is designed and studied with consideration of the ohmic loss on the cavity wall. To ensure maximum excitation factor at the fifth harmonic, the operation mode is chosen to be $TE_{5,1,1}$. It is shown that by enabling the fifth harmonic oscillation, an output frequency of 283 *GHz* can be achieved with an external magnetic field as low as 2.96 *T*. With consideration of the cavity wall loss, a stable output power of 1.003 *kW* is obtained while the ohmic loss power amounts to 4.914 *kW* due to the adoption of a whispering gallery mode. The values of the diffraction quality factor and the ohmic quality factor obtained from the hot cavity simulations agree with the ones from cold cavity analysis. The remaining part of this paper is organized as follows: Part 2 provides the design and the cold cavity analysis of the LOG with $TE_{5,1,1}$ as the operation mode. Part 3 shows the hot cavity simulation result and its comparison with that obtained from the cold cavity analysis. Part 4 draws conclusion and suggests the future work.

2. Gyrotron design and cold cavity analysis

The structure of the beam-wave interaction cavity is shown in Figure 1, which is consisted of an input conical cavity, a smooth cylindrical cavity and an output conical cavity. The input taper angle θ_{in} and the output taper angle θ_{out} are chosen as $4.8°$ and $2.8°$, respectively. The cavity radius is calculated based on the cyclotron resonance condition [7]. The other structural parameters are optimised to provide a relatively large diffraction quality factor. An electron beam with a voltage of 250 *kV*, a maximum beam current of 10 *A*, and a pitch factor of 2 is chosen in this study [4].
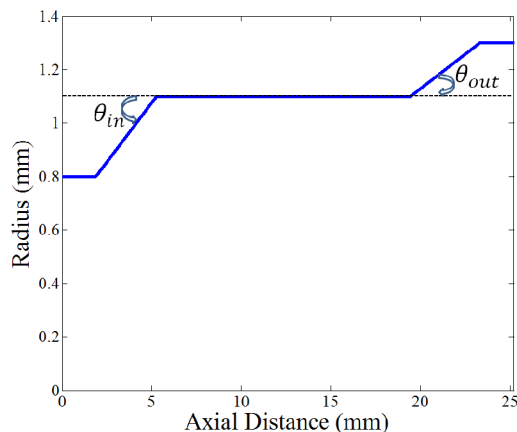

Fig. 1 Schematic view of the beam-wave interaction cavity

The operation frequency f and diffraction quality factor Q_d of the above cavity are calculated with an existing cold cavity code [8] to be 283.58 *GHz* and 12654, respectively. The ohmic quality factor is calculated to be 3390 by the following expression [4-6]:

$$Q_\Omega = (R_w / \delta)(1 - m^2 / \mu_{m,n}'^2) \tag{1}$$

in which R_w is the beam-wave interaction cavity radius and $\delta = \sqrt{1/\pi f \mu \varepsilon}$ is the skin depth. $\varepsilon = 5.99 \times 10^{-7} S/m$ and $\mu = 4\pi \times 10^{-7} H/m$ are the conductivity and permeability of the oxygen-free copper. The ohmic quality factor in the designed cavity is smaller than the diffraction quality factor, meaning that more than half of the extracted power from the electrons will be converted to the cavity wall loss. Such situation is predictable since the whispering gallery mode TE$_{5,1,1}$ is used where the field maxima is very close to the cavity wall. The total quality factor Q is calculated by the following equation:

$$Q = Q_d \cdot Q_\Omega / (Q_d + Q_\Omega) \tag{2}$$

3. Numerical simulation

Based on the above parameters, a 3D model is built in the FDTD-PIC code MAGIC Tool Suite 2007 [9]. The oxygen-free copper is set as the cavity material to take into consideration of the ohmic loss. From the cold cavity analysis, the starting oscillation current of TE$_{5,1,1}$ mode is lower than the neighbouring modes when the magnetic field is chosen between 2.94 *T* to 2.98 *T*. The numerical simulation result, when the external magnetic field is 2.96 *T*, is shown below. The beam current is chosen as 0.3 *A*.

The output time signal is recorded at the output aperture of the cavity before a Fast Fourier Transformation (FFT) is applied, as shown in Figure 2. The output spectrum is pure with only one peak at 283.3271 *GHz* which also suggests a single mode operation without mode competition. Thus the LOG is superior in supporting the electron cyclotron resonance at high harmonic numbers ($s > 3$) than its small-orbit counterpart.
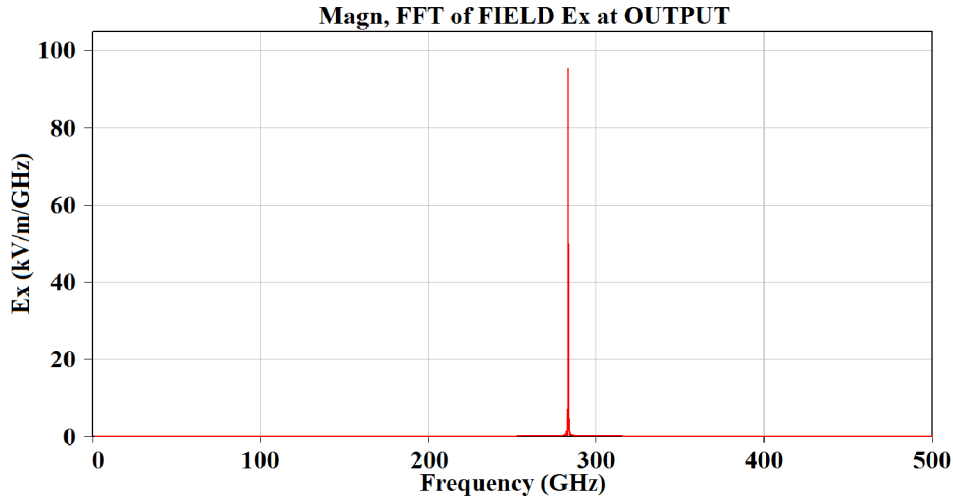
Fig. 2 Spectrum of the output time signal

To identify the operation mode, the transverse magnetic field distribution at 35.250 *ns* is recorded at the middle intersection of the beam-wave interaction cavity, as shown in Fig. 3. A total of 10 peaks can be seen in the azimuthal direction while just one peak is identified in the radial direction, meaning that the operation mode is $TE_{5,1}$.
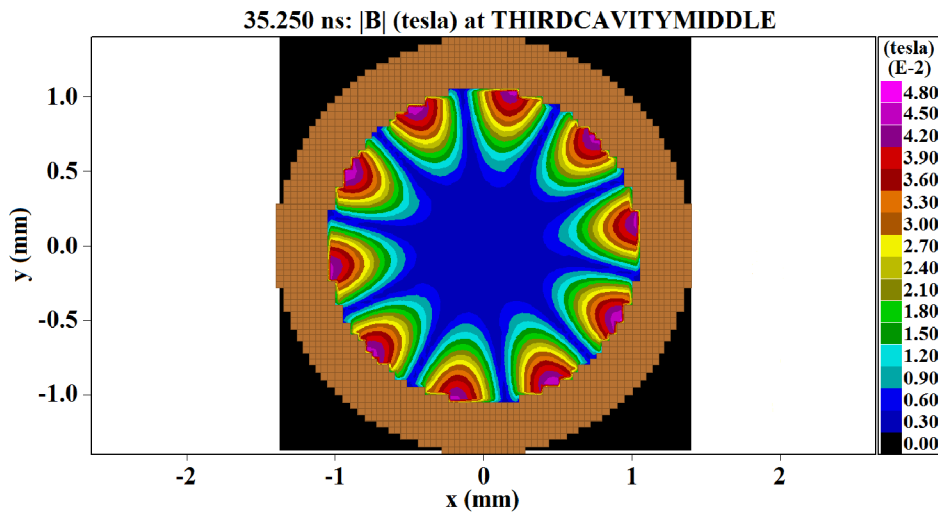

Fig. 3 Transverse magnetic field distribution

Fig. 4 provides the axial electric field distribution at 35.250 *ns*. It can be seen that there is just one peak in the axial direction, meaning that the axial index of the operation mode is 1. From the above observation, the operation mode inside the beam-wave interaction cavity is $TE_{5,1,1}$ mode.
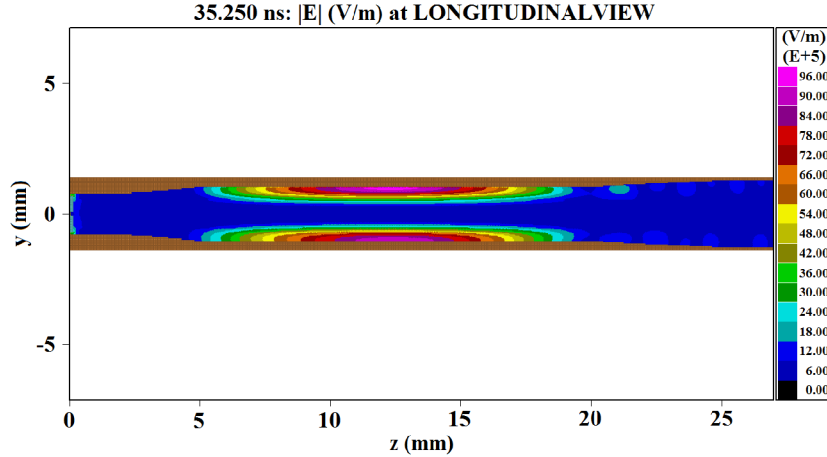
Fig. 4 Axial electric field distribution

The time-dependent variations of the output power (P_d), ohmic loss power (P_Ω) and the total energy storage (*W*) are shown in Fig. 5. It can be interpreted that the beam-wave interaction stabilized at 30 *ns* with an output power of 1.003 *kW* and an ohmic loss power of 4.914 *kW*. The total energy storage inside the whole cavity stabilized at 8.35 μJ. Thus the diffraction quality factor Q_d and the ohmic quality factor Q_Ω can be calculated from

$$Q_d = 2\pi f \cdot \frac{W}{P_d} \tag{3}$$

$$Q_\Omega = 2\pi f \cdot \frac{W}{P_\Omega} \tag{4}$$

The resultant Q_d and Q_Ω are 14818 and 3024, respectively, which is in reasonable agreement with the previous cold cavity analysis. The discrepancy can be explained by the limited accuracy of the staircase representation of the cavity structure in FDTD-PIC codes and the overbunching of the electron beam [10].
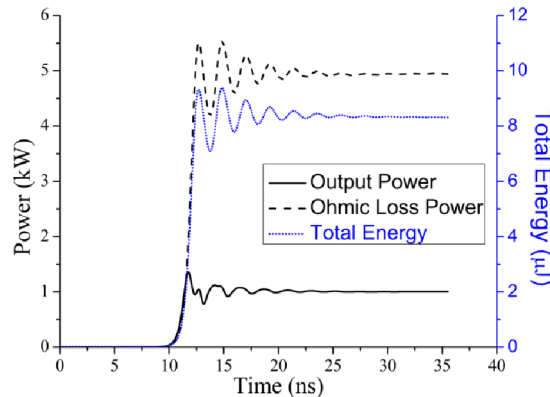

Fig. 5 The output power, ohmic loss power and total energy storage variation with time

4. Conclusion

In this paper, a fifth-harmonic LOG operating at 283.3 *GHz* is designed and numerically investigated. With the assistance of 3D FDTD-PIC code MAGIC, the operation of the designed LOG is characterized. By enabling high harmonic operation, the required external magnetic field strength can be greatly reduced, which is an essential feature in the development of THz gyrotrons. The cold cavity analysis and the hot cavity simulation results reasonably agree with each other. By using the design procedure and the analysis method in this paper, even higher harmonics operation of the LOG can be obtained.

Acknowledgement

References

[1] T. Idehara, S. Mitsudo, M. Ui, et. al.. "Development of frequency tunable gyrotrons in millimeter to submillimeter wave range for plasma diagnostics". *J. Plasma Fusion Res. Series,* 3, 407-410 (2000).

[2] V. Bajaj, C. Farrar, M. Hornstein, et. al.. "Dynamic nuclear polarization at 9T using a novel 250GHz gyrotron microwave source". *Journal of Magnetic Resonance,* 160, 85-90 (2003).

[3] J. Federici and L. Moeller. **"**Review of terahertz and subterahertz wireless communications". *Journal of Applied Physics,* 107, 111101-111101-22 (2010).

[4] V. L. Bratman, A. E. Fedotov, Y. K. Kalynov, et. al.. "Moderately relativistic high-harmonic gyrotrons for millimeter/submillimeter wavelength band: Special Issue on Cyclotron Resonance Masers and Gyrotrons". *IEEE Transactions on Plasma Science,* 27, 456-461 (1999).

[5] T. Idehara, I. Ogawa, S. Mitsudo, et. al.. "A high harmonic gyrotron with an axis-encircling electron beam and a permanent magnet". *IEEE Transactions on Plasma Scienc*e, 32, 903-909 (2004).

[6] K. Irwin, W. Destler, W. Lawson, et. al.. "Second generation, high-power, fundamental mode large-orbit gyrotron experiments". *Journal of Applied Physics,* 69, 627-631 (1991).

[7] F. Li, W. He, A. W. Cross, et. al.. "Design and simulation of a~ 390 GHz seventh harmonic gyrotron using a large orbit electron beam". *Journal of Physics D: Applied Physics,* 43, 155204 (2010).

[8] Hongfu Li, Zhonglian Xie, Wenxiang Wang, et. al.. "A 35 GHz Low-Voltage Third-Harmonic Gyrotron With a Permanent Magnet System". *IEEE Transactions on Plasma Science,* 31, 264-271 (2003).

[9] Alliant Techsystems Operations (ATK), *Magic Tool Suite User Help Document* (2007).

[10] M. V. Kartikeyan, E. Borie, and M. Thumm. *Gyrotrons: High-Power Microwave and Millimeter Wave Technology,* Spriner (2004).